Predicted Prognosis of Patients with Pancreatic Cancer by Machine Learning

Seiya Yokoyama[1], Taiji Hamada[1], Michiyo Higashi[1], Kei Matsuo[1], Kosei Maemura[2,3], Hiroshi Kurahara[3], Michiko Horinouchi[1], Tsubasa Hiraki[1], Tomoyuki Sugimoto[4], Toshiaki Akahane[1], Suguru Yonezawa[1], Marko Kornmann[5], Surinder K. Batra[6], Michael A. Hollingsworth[7], and Akihide Tanimoto[1]

ABSTRACT

Purpose: Pancreatic cancer remains a disease of high mortality despite advanced diagnostic techniques. Mucins (MUC) play crucial roles in carcinogenesis and tumor invasion in pancreatic cancers. MUC1 and MUC4 expression are related to the aggressive behavior of human neoplasms and a poor patient outcome. In contrast, MUC2 is a tumor suppressor, and we have previously reported that MUC2 is a favorable prognostic factor in pancreatic neoplasia. This study investigates whether the methylation status of three *mucin* genes from postoperative tissue specimens from patients with pancreatic neoplasms could serve as a predictive biomarker for outcome after surgery.

Experimental Design: We evaluated the methylation status of MUC1, MUC2, and MUC4 promoter regions in pancreatic tissue samples from 191 patients with various pancreatic lesions using methylation-specific electrophoresis. Then, integrating these results and clinicopathologic features, we used support vector machine-, neural network-, and multinomial-based methods to develop a prognostic classifier.

Results: Significant differences were identified between the positive- and negative-prediction classifiers of patients in 5-year overall survival (OS) in the cross-validation test. Multivariate analysis revealed that these prognostic classifiers were independent prognostic factors analyzed by not only neoplastic tissues but also nonneoplastic tissues. These classifiers had higher predictive accuracy for OS than tumor size, lymph node metastasis, distant metastasis, and age and can complement the prognostic value of the TNM staging system.

Conclusions: Analysis of epigenetic changes in *mucin* genes may be of diagnostic utility and one of the prognostic predictors for patients with pancreatic ductal adenocarcinoma.

Introduction

Despite improvements in diagnostic tools and treatments, patients with pancreatic ductal adenocarcinoma (PDAC) have a poor clinical outcome. At the time of diagnosis, most patients with PDAC are in advanced stages because the anatomic location of the pancreas and lack of specific symptoms hamper early detection. Easy infiltration to the surrounding organs and early distant metastasis, even from a small primary tumor <2 cm in diameter, enhances the stage progression (1). Moreover, PDAC is sometimes difficult to distinguish from other pancreatic diseases, such as chronic pancreatitis, even when endoscopic, ultrasound-guided, fine-needle aspiration is performed (2–4). Indolent tumors such as intraductal papillary mucinous neoplasms (IPMN) also occur in the pancreas and sometimes transform to invasive cancer with a poor outcome (5–8). Currently, IPMNs are the most common cystic neoplasm of the pancreas and are classified into gastric, intestinal, pancreatobiliary, and oncocytic types (9, 10). A recent study has demonstrated that the morphologic subtype of IPMN is an independent prognostic factor (8). The overall 5-year survival rate for all diagnosed patients with PDAC is presently only 13% in Japan. Unfortunately, only 10%–20% patients present with resectable disease at diagnosis of PDAC (11). Five-year survival with tumor removal alone is generally less than 10%. After resection, the use of adjuvant chemotherapy doubled 5-year survival to around 16%–21% (12); however, it can be increased to 38.6% after a successful resection at stage IIA (13–16). Therefore, it is essential to identify effective biomarkers to enable early diagnosis and precisely predict the prognosis to recommend additional neoadjuvant and adjuvant therapies

Mucins (MUC) play crucial roles in carcinogenesis and tumor invasion in pancreatic tumors. The MUC gene product is posttranslationally modified, most likely, through extensive O-glycosylation. MUC1 and MUC4 are large membrane-bound glycoproteins that are translated as single polypeptides. These mucins undergo intracellular autocatalytic proteolytic cleavage into two subunits that form stable noncovalent heterodimers that are transported to the cell surface. MUC2 is gel-forming secretory mucin that is expressed in many organs, including the colon, small intestine, and respiratory tract (17–19). MUC1 contributes to oncogenesis by promoting the loss of epithelial cell polarity, promoting growth and survival pathways, activating receptor tyrosine kinase signaling pathways, and conferring resistance to the stress-induced cell death pathway (20, 21). MUC1 cytoplasmic domain has been implicated in the regulation of the Wnt–β-catenin, p53, and NF-κB pathways, all of which are linked to tumor progression (19, 22). MUC4 plays an important role in

[1]Department of Pathology, Graduate School of Medical and Dental Sciences, Kagoshima University, Kagoshima, Japan. [2]Center for the Research of Advanced Diagnosis and Therapy of Cancer, Graduate School of Medical and Dental Sciences, Kagoshima University, Kagoshima, Japan. [3]Department of Digestive Surgery, Breast and Thyroid Surgery, Graduate School of Medical Sciences, Kagoshima University, Kagoshima, Japan. [4]Graduate School of Science and Engineering (Science), Kagoshima University, Kagoshima, Japan. [5]Department of General and Visceral Surgery, University of Ulm, Ulm, Germany. [6]Department of Biochemistry and Molecular Biology, Eppley Institute for Research in Cancer and Allied Diseases, University of Nebraska Medical Center, Omaha, Nebraska. [7]Fred and Pamela Buffet Cancer Center, Eppley Institute for Research in Cancer, University of Nebraska Medical Center, Omaha, Nebraska.

Note: Supplementary data for this article are available at Clinical Cancer Research Online (http://clincancerres.aacrjournals.org/).

Corresponding Author: Michiyo Higashi, Field of Oncology, Kagoshima University Graduate School of Medical and Dental Sciences, 8-35-1 Sakuragaoka, Kagoshima 890-8544, Japan. Phone: 819-9275-5270; Fax: 819-9265-7235; E-mail: east@m2.kufm.kagoshima-u.ac.jp

Clin Cancer Res 2020;26:2411–21

doi: 10.1158/1078-0432.CCR-19-1247

Translational Relevance

Pancreatic cancer remains a disease of high mortality despite advanced diagnostic techniques. This study investigates whether the methylation status of three *mucin* genes from postoperative tissue specimens from patients with pancreatic neoplasms could serve as a predictive biomarker for outcome after surgery. We evaluated the methylation status of MUC1, MUC2, and MUC4 promoter regions in 300 pancreatic non- and neoplastic tissues samples from 191 patients with various pancreatic lesions using methylation-specific electrophoresis. Furthermore, integrating these results and clinicopathologic features, we used support vector machine-, neural network-, and multinomial-based methods to develop a prognostic classifier. Multivariate analysis revealed that these prognostic classifiers were independent prognostic factors analyzed by not only neoplastic tissues but also nonneoplastic tissues. Analysis of epigenetic changes in *mucin* genes may be of diagnostic utility and one of the prognostic predictors for patients with pancreatic ductal adenocarcinoma.

epithelial cell proliferation and differentiation by inducing specific phosphorylation of ERBB2 and enhancing the expression of the cyclin-dependent kinase inhibitor p27, which inhibits cell-cycle progression (23, 24). The loss of *MUC2* might compromise signaling that contributes to epithelial differentiation and proliferation through contact with membrane-bound mucins or alters the differentiation program of the intestinal mucosa, resulting in an increased probability of tumor formation (25, 26). In our previous studies, we used pancreatic tissue samples and several cancer cell lines to demonstrate that MUC1, MUC2, and MUC4 expression of mRNA and/or protein are regulated by hypoxia and/or DNA demethylation (27–30). However, it has not been reported how that DNA methylation of promoter region effect for intracellular localization of these three mucin proteins. Furthermore, MUC1 and MUC4 hypomethylation status are statistically associated with the development of distant metastasis, tumor stage, and overall survival (OS) for patients with PDAC (31–34).

In machine learning, state-of-the-art classification algorithms, such as support vector machines (SVM), neural networks (NNET), or multinomial prediction models, are used for classification and regression analysis (35–37). Recently, several studies shows that in breast cancer, nasopharyngeal carcinoma, and non–small cell lung cancer, several supervised learning methods, such as decision trees using data of cDNA or tissue microarray refine prognosis (38–41). However, it was not reported whether these machine learning models could use DNA methylation status to predict the outcome of patients with pancreatic tumors.

Therefore, the aim of this study was to develop a machine learning–based prognostic classifier to predict OS with pancreatic cancers by integrating multiple DNA methylation statuses of three *mucin* genes. In this study, we increased the number of patients that were evaluated from that of our previous study and performed a sequential analysis of mucin promoter–associated CpGs by methylation-specific electrophoresis (MSE) analysis.

Materials and Methods

Cell lines and culture

Human pancreatic cancer cell lines BxPC3, HPAF2, and Panc1; human colon adenocarcinoma cell lines Caco2 and LS174T; and human lung adenocarcinoma cell lines A427 and NCI-H292 were obtained from the ATCC. HPAF2, LS174T, and Caco2 cells were cultured in Eagle Minimum Essential Medium (Sigma); PANC1 and A427 cells were cultured in DMEM (Sigma); and BxPC3 and NCI-H292 cells were cultured in RPMI1640 medium (Sigma). The media were supplemented with 10% FBS (Invitrogen), 100 U/mL of penicillin (Sigma), and 100 μg/mL streptomycin (Sigma). Hypoxic culture conditions were achieved with a multigas incubator containing a gas mixture of 94% N_2, 5% CO_2, and 1% O_2 (ASTEC).

Clinical samples

Pancreatic tissue samples

We obtained 300 surgically resected tissues (approximately $2 \times 2 \times 2$ mm in size) from neoplastic and nonneoplastic areas of 191 patients. **Table 1** summarizes the clinicopathologic features of the 114 neoplastic samples and 186 nonneoplastic samples (including 109 paired samples). We collected 125 patient samples (48 neoplastic samples and 120 nonneoplastic samples, including 43 paired samples) from Kagoshima University (Kagoshima, Japan), from August 2007 to May 2014 and 66 patient samples (all nonneoplastic and neoplastic paired samples) from Ulm University (Ulm, Germany), from February 2001 to February 2013. The nonneoplastic tissues were collected around the resection stump. These samples were checked for pathologic diagnosis using intraoperative frozen and formalin-fixed paraffin-embedded (FFPE) tissue sections. On the other hand, neoplastic tissues were macroscopically collected, processed for FFPE tissue sections, and diagnosed by a board-certified pathologist. The clinical features used in this study were TNM, age, American Society of Anesthesiologists (ASA) physical status classification score, the presence or absence of comorbidities, and preoperative chemotherapy. Almost all patients had not undergone radiotherapy before surgery; therefore, we removed the information about radiotherapy in statistical analysis.

Extraction and quantification of mRNA

tRNA was extracted from the cell lines, human pancreatic tissues, and pancreatic juices using an RNeasy Mini Kit (Qiagen). Then, the tRNA (1 μg) was reverse transcribed with a High-Capacity RNA-to-cDNA Kit (Applied Biosystems), and real-time reverse transcription-PCR was performed on a Roche LightCycler 96 System using FastStart Essential DNA Green Master (Roche). Gene expression was normalized to the β-actin mRNA level in each sample. The data were normalized using the NCI-H292 cell line, and the A427 cell line was used as a negative control. Primer sets are shown in previously study (31, 33, 34).

Extraction of DNA and bisulfite modification

DNA from the cell lines, pancreatic tissues, and pancreatic juices was extracted using a DNeasy Tissue System (Qiagen). The bisulfite modification of the genomic DNA was carried out using an EpiTect Bisulfite Kit (Qiagen). The purification of PCR products was carried out using a Wizard SV Gel and PCR Clean-Up System (Promega KK; refs. 31, 33, 34).

MSE analysis

MSE analysis was performed using previously described methods. Briefly, the target DNA fragments were amplified by nested PCR using bisulfite-treated DNA with the primer sets detailed in previously study (31–34). Then, the PCR products were run on a polyacrylamide gel with a linear denaturant gradient at

Table 1. Patient and tumor characteristics in the study.

Age				
Median	(Male/female)	66, (65.3/66.8)	Year	
Observation period (OP)				
Median	(Male/female)	22.4, (23.5/21.2)	Months	
ASA score				
Median	(Male/female)	2, (2/2)		
		Number of cases (non-/neoplastic)	OP Median	Age Median
Stage	Non	30 (29/20)	38.4	59.2
	IA	18 (17/2)	22.1	67.3
	IB	12 (12/4)	25.4	66.3
	IIA	36 (35/26)	16.2	65.8
	IIB	64 (63/43)	19.6	69.1
	III	3 (3/3)	14.3	68.3
	IV	6 (5/6)	11.5	66.5
	NA	22 (22/10)	15	54
T	0	21 (20/11)	24.4	59.3
	1	20 (19/3)	25.1	67.5
	2	17 (17/4)	23.6	66.6
	3	98 (96/73)	17.3	67.8
	4	4 (3/4)	13.8	68.3
	NA	31 (31/19)	60.8	57.9
N	0	90 (86/46)	20.3	64.4
	1	69 (68/48)	19.2	69.2
	NA	31 (31/19)	60.8	57.9
M	0	153 (149/88)	19.8	66.5
	1	6 (5/6)	11.5	66.5
	NA	32 (32/20)	60.8	58.7
		Number of cases (non-/neoplasm)		
		Presence	Absence	
Comorbidities		84 (81/62)	87 (87/43)	
Preoperative chemotherapy		130 (127/64)	41 (41/41)	

60°C at 70 V for 14 hours using a D-Code Universal Mutation Detection System (Bio-Rad Laboratories). Band intensity was quantified by Image J Software (NIH, Bethesda, MD). The demethylation index was calculated as the proportion of the highest band intensity/total band intensity of the sample. Subsequently, the demethylation index for each sample was normalized using data from a hypomethylated and hypermethylated cell line. Cell lines with hyper- and hypomethylation of MUC1 and MUC4 (Caco2 and LS174T, respectively) were used as control standards. We performed MSE analysis on duplicate samples.

Statistical analysis and prediction model construction

Data were analyzed using the "R" computing environment version 3.5.2 (42). The normality of the data distribution was evaluated using the Kolmogorov–Smirnov test. Differences between groups were analyzed using Welch *t* test. A nonparametric test of group difference was performed using the Mann–Whitney *U* test. Survival rate analysis was evaluated using Cox proportional hazards model. Hierarchical cluster analysis on a set of dissimilarities was performed using the reproduce package of R. A $P < 0.05$ was considered statistically significant.

Construction of an SVM classifier

We constructed the SVM classifier using the kernlab package, including the ksvm function (37). Methylation analyzed data mining, such as scaling and centering, were performed using the scale function. C-classification with the linear vanilladot kernel, Gaussian radial basis function, polynomial kernel, hyperbolic tangent kernel, Bessel function of the first kind kernel, Laplace radial basis kernel, and ANOVA radial basis kernel were used in training and predicting. In this study, we used default hyperparameters and cost of constraints violation for preparing the prediction models. The quality of the model was assessed using 5-fold cross-validation of the training data.

Construction of an NNET and a multinomial classifier

Neural networks provide a flexible, nonlinear extension of multiple logistic regressions to perform classification, pattern recognition, and prediction modeling. The nnet package, including the nnet function, was used to construct an NNET classifier (43). The classifier parameters were set with a weight decay of 0.1, 2 units in the hidden layer and 100 as the maximum number of iterations. To construct the multinomial log-linear model (MU) via the NNET classifier, the multinom function was employed.

Ethics statement

This study was conducted in accordance with the guiding principles of the Declaration of Helsinki. The ethical committees of both Kagoshima University Hospital (Kagoshima, Japan) and Ulm University Hospital (Ulm, Germany) approved sample collection, and informed written consent was obtained from each patient. All studies using human materials in this article were approved by the Ethical Committee of Kagoshima University Hospital (Kagoshima, Japan; revised 20–82, revised 22–127, and 26-145).

Results

Mucin expression characteristic analysis and prognosis differential

Unsupervised hierarchical clustering analysis was performed for three mucin gene expression datasets including neoplastic and nonneoplastic pancreatic regions (**Fig. 1A**). The samples were divided into two clusters according to the clustering results. Cluster 1 showed a significantly higher expression level of the three *mucin* genes as MUC1, MUC2, and MUC4 compared with cluster 2 (all $P < 0.001$; **Fig. 1B**). Cluster 1 also demonstrated a significantly poorer prognosis than cluster 2 (HR = 0.52; $P < 0.001$; **Fig. 1C**). As shown in **Table 2**, this clustering analysis showed the same result in the nonneoplastic tissue ($P < 0.001$). In nonneoplastic region, cluster 1 showed a significantly poorer prognosis than cluster 2 (HR = 0.49; $P = 0.012$; Supplementary Fig. S1A). Similarly, cluster 1 showed a significantly poorer prognosis than cluster 2 in the neoplastic region (HR = 0.53; $P = 0.032$; Supplementary Fig. S1B).

Mucin DNA methylation characteristics and prognosis differential

Unsupervised hierarchical clustering analysis was performed for three mucin gene methylation datasets including neoplastic and nonneoplastic pancreatic regions (**Fig. 2A**). According to the clustering results, the samples were divided into four clusters. Cluster 1 showed a significantly higher hypomethylation status of *MUC1* and *MUC4* genes than the other clusters ($P = 0.003$ and $P < 0.001$, respectively; **Fig. 2B**). Cluster 1 also demonstrated a significantly higher expression level of MUC1, MUC2, and MUC4 than the other clusters ($P = 0.004$, $P = 0.002$, and $P = 0.015$, respectively; Supplementary Fig. S2). Furthermore, cluster 1 demonstrated a significantly poorer prognosis than the other clusters (HR = 0.33; $P = 0.012$; **Fig. 2C**). As shown in **Table 2**, this clustering analysis did not identify a significant difference in the nonneoplastic ratio between Cluster 1 and the other clusters ($P < 0.357$). In the nonneoplastic regions, cluster 1 showed a significantly poorer prognosis than the other clusters (HR = 0.49; $P = 0.010$; Supplementary Fig. S3A). Similarly, in the neoplastic regions, cluster 1 also showed a significantly poorer prognosis than the other clusters (HR = 0.48; $P = 0.014$; Supplementary Fig. S3B).

Prediction model classifier and survival in the cross-validation test

SVM prediction model and performance evaluation

In the leave-one-out cross-validation (LOOCV) test, the SVM classifier model by C-classification with ANOVA RBF kernel function using the dataset for DNA methylation of three mucins, including both nonneoplastic and neoplastic regions, showed good classification for prognosis after surgery (**Fig. 3A**). In addition, ANOVA RBF kernel as a nonlinear kernel showed the best classification than the other kernels, including linear kernel (Supplementary Table S1). This SVM classification showed no significant differences in the nonneoplastic ratio between high-risk positive and negative groups (Supplementary Table S2). In nonneoplastic regions, the high-risk group indicated by SVM showed a significantly poorer prognosis after surgery than the negative group (**Fig. 3B**). Similarly, in neoplastic regions, the high-risk group indicated by SVM also showed a significantly poorer prognosis after surgery than the negative group (**Fig. 3C**). In univariate analysis, patients who were classified as positive by the SVM model

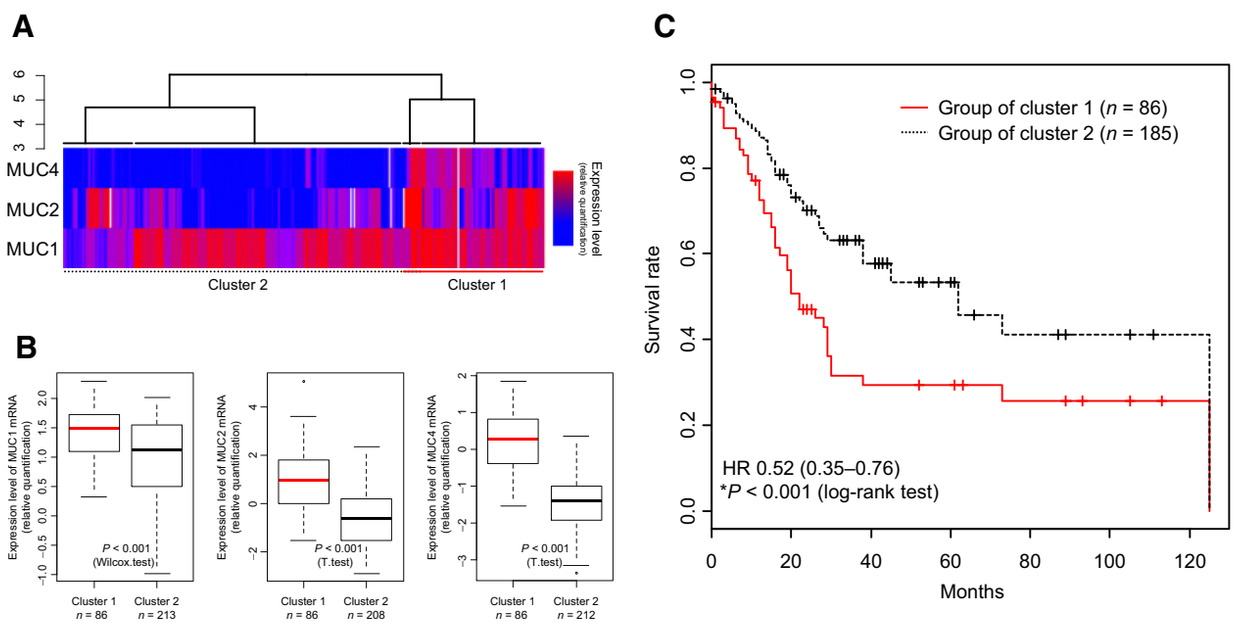

Figure 1.

Cluster analysis of the mRNA expression level of *mucin* genes. **A,** Tree generated by cluster analysis of neoplastic and nonneoplastic pancreas tissues for the expression levels of MUC1, MUC2, and MUC4 mRNAs compared with each control cell line. High mRNA expression levels are indicated in red and low levels in blue. **B,** Comparison of expression levels of MUC1, MUC2, and MUC4 mRNAs between cluster 1 and cluster 2. Expression levels show relative quantification (log_{10}). **C,** Cox proportional hazard regression analysis of a comparison between cluster 1 and cluster 2. Red solid line, cluster 1; black dashed line, cluster 2.

Table 2. Clustering analysis result and clinicophathologic data.

1. mRNA data clustering analysis					2. Methylation data clustering analysis				
		Cluster 1	**Cluster 2**	***P***			**Cluster 1**	**Others**	***P***
Age	Mean ∓ SD	66.93 ∓ 11.2	65.74 ∓ 9.5	0.756	Age	Mean ∓ SD	65.63 ∓ 10.6	66.32 ∓ 10.7	0.632
	Observation period (OP)					Observation period (OP)			
	Mean ∓ SD	23.72 ∓ 23.4	23.9 ∓ 28.5	0.267		Mean ∓ SD	30.04 ∓ 34.1	21.29 ∓ 19.8	0.709
	Tissue region (*n*)					Tissue region (*n*)			
Nonneoplasm		36	150	<0.001	Nonneoplasm		49	137	0.357
Neoplasm		63	51		Neoplasm		36	78	
ASA score	Mean ∓ SD	1.81 ∓ 0.9	2.33 ∓ 0.8	0.142	ASA score	Mean ∓ SD	2.57 ∓ 0.6	1.73 ∓ 0.8	<0.001
Stage (*n*)	Non	12	37	<0.001	Stage (*n*)	Non	14	35	0.018
	IA	0	19			IA	1	18	
	IB	3	13			IB	5	11	
	IIA	22	39			IIA	25	36	
	IIB	43	63			IIB	28	78	
	III	3	3			III	4	2	
	IV	3	8			IV	2	9	
	NA	1	31			NA	6	26	
T (*n*)	0	4	27	0.004	T (*n*)	0	2	29	<0.001
	1	2	20			1	1	21	
	2	7	14			2	5	16	
	3	62	107			3	55	114	
	4	3	4			4	4	3	
	NA	9	41			NA	18	32	
N (*n*)	0	30	102	0.002	N (*n*)	0	35	97	0.413
	1	48	70			1	32	86	
	NA	9	41			NA	18	32	
M (*n*)	0	75	162	0.115	M (*n*)	0	64	173	0.29
	1	3	8			1	2	9	
	NA	9	43			NA	19	33	
Comorbidities (*n*)					Comorbidities (*n*)				
	Presence	54	89	0.026		Presence	58	85	<0.001
	Absence	32	98			Absence	21	109	
Preoperative chemotherapy (*n*)						Preoperative chemotherapy (*n*)			
	Presence	42	149	<0.001		Presence	30	161	<0.001
	Absence	44	38			Absence	49	33	

were associated with a significantly poorer OS. Multivariate Cox regression analysis after adjustment for clinicopathologic variables, such as ASA score, preoperative chemotherapy, comorbidities, and TNM stage, revealed that the SVM classifier remained a powerful and independent prognostic factor for OS in the LOOCV test (Supplementary Table S3). Following several k-fold cross-validation tests, we performed 3-, 4-, and 10-fold cross-validations in this study. The SVM classifier showed good classification for prognosis after surgery in both regions (Supplementary Fig. S4; **Table 3**). Multivariate and/or univariate analysis revealed that SVM classifier was an independent prognostic factor (Supplementary Table S3).

NNET prediction model and performance evaluation

In the LOOCV test, the NNET classifier model using the dataset for DNA methylation of three mucins, including both nonneoplastic and neoplastic regions, showed good classification for prognosis after surgery (**Fig. 3D**). This NNET classification showed no significant difference in the nonneoplastic ratio between high-risk positive and negative groups (Supplementary Table S2). In nonneoplastic regions, the high-risk group indicated by NNET showed a significantly poorer prognosis after surgery than the negative group (**Fig. 3E**). Similarly, in neoplastic regions, the high-risk group indicated by NNET also showed a significantly poorer prognosis after surgery than the negative group (**Fig. 3F**). In univariate analysis, patients who were classified as high-risk positive by the NNET model were associated with a significantly poorer OS. Multivariate Cox regression analysis after adjustment for clinicopathologic variables, such as ASA score, preoperative chemotherapy, comorbidities, and TNM stage, revealed that the NNET classifier remained a powerful and independent prognostic factor for OS in the LOOCV test (Supplementary Table S3). After several k-fold cross-validation tests, the NNET classifier showed a tendency toward good classification for prognosis after surgery in both nonneoplastic and neoplastic regions (Supplementary Fig. S4; Supplementary Table S3). Multivariate and/or univariate analysis

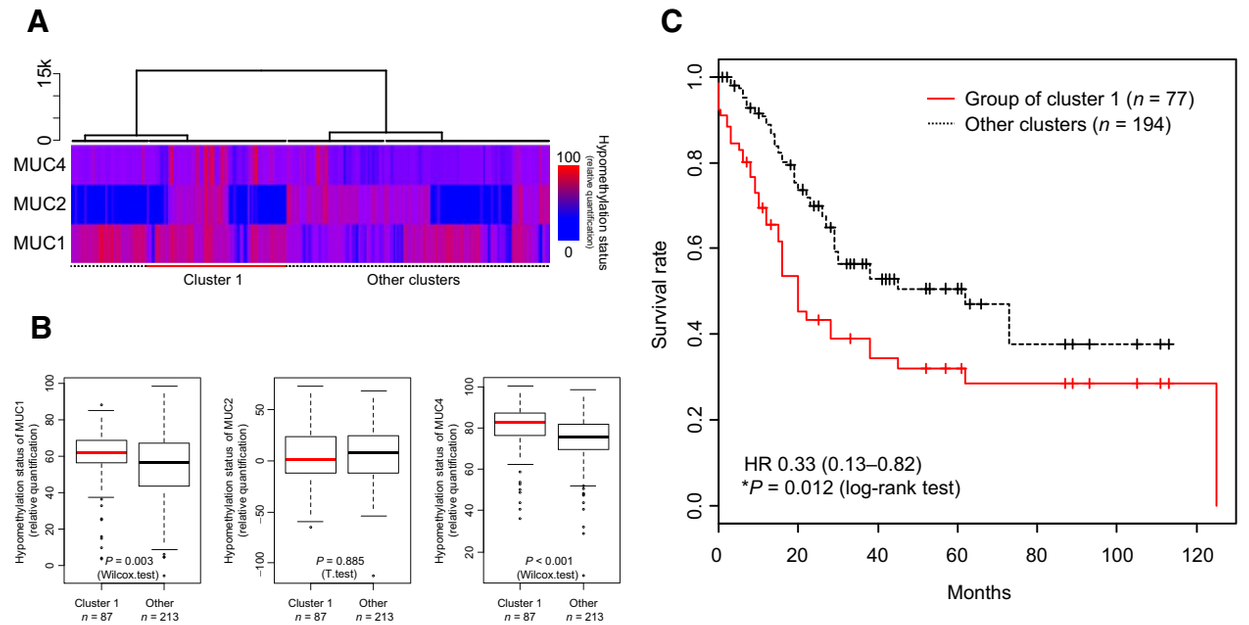

Figure 2.

Cluster analysis of the methylation status of *mucin* genes. **A,** Tree generated by cluster analysis of neoplastic and nonneoplastic pancreas tissues from the methylation status of *MUC1, MUC2*, and *MUC4* genes evaluated by MSE analysis. Hypomethylation is indicated in red and hypermethylation in blue. **B,** Comparison of the methylation status of *MUC1, MUC2*, and *MUC4* genes between cluster 1 and the other clusters. **C,** Cox proportional hazard regression analysis on a comparison between cluster 1 and other clusters. Red solid line, cluster 1; black dashed line, other clusters.

showed that NNET classifier was independent from prognostic factors (Supplementary Table S3).

MU prediction model and performance evaluation

In the LOOCV test, the MU classifier model using the dataset for DNA methylation of three mucins, including both nonneoplastic and neoplastic regions, did not show good classification for prognosis after surgery (**Fig. 3G**). However, this MU classification revealed a significant difference in the nonneoplastic ratio between the high-risk positive and negative groups ($P < 0.043$; Supplementary Table S2). In neoplastic regions, the negative group indicated by MU showed a significantly poorer prognosis after surgery than the high-risk group (**Fig. 3H**), but not in nonneoplastic regions (**Fig. 3I**). The multivariate Cox regression analysis after adjustment for clinicopathologic variables such as TNM stage revealed that the MU classifier was an independent prognostic factor for OS in the LOOCV test. However, in univariate analysis, patients who were positive according to the MU model were not associated with significantly poorer OS (Supplementary Table S3). In k-fold cross-validation test, the MU classifier demonstrated good classification ability for prognosis after surgery in the neoplastic region but not in nonneoplastic region (Supplementary Fig. S4; Supplementary Table S3).

Evaluation of prediction models using training cohort in the test cohort

To evaluate whether the prediction models constructed using test datasets could detect high-risk groups in other training dataset, we split the total dataset into two groups: training and test datasets. These two groups showed almost similar distribution in biological analysis results and clinicopathologic features (shown in Supplementary Table S4). SVM and NNET classifiers exhibited significantly good classification ability for prognosis after surgery in not only the neoplastic region but also the nonneoplastic region (**Fig. 4**). Multivariate and/or univariate analysis revealed that these classifiers were independent from prognostic factors (shown in Supplementary Table S3). The MU classifier demonstrated good classification ability for prognosis after surgery in the neoplastic region but not in nonneoplastic region (**Fig. 4G–I**).

Discussion

PDAC is an aggressive malignancy with an extremely poor prognosis due to delayed diagnosis, early metastasis, and resistance to most cytotoxic agents (1, 13). Thus, it is critical to establish new diagnostic, prognostic, and therapeutic biomarkers. It has been previously demonstrated that mucin gene expression (including MUC1, MUC2, MUC3, MUC4, and MUC5AC) is regulated by DNA methylation at promoter regions in cancer cell lines (27–30). In this study, scientific computer prediction model–based SVM and NNET methods were able to classify between a good and poor prognosis after surgery on pancreatic cancers. These predicted models were constructed from the methylation status of three mucin genes (*MUC1, MUC2*, and *MUC4*), which had all previously demonstrated a significant difference in mucin expression levels in pancreatic cancers.

To construct a clinical test to predict prognosis after surgery, we used an expression dataset including nonneoplastic and neoplastic pancreatic tissues. To determine whether the expression levels of MUC1, MUC2, and MUC4 mRNA could distinguish a poor prognosis from data, we performed unsupervised hierarchical clustering analysis

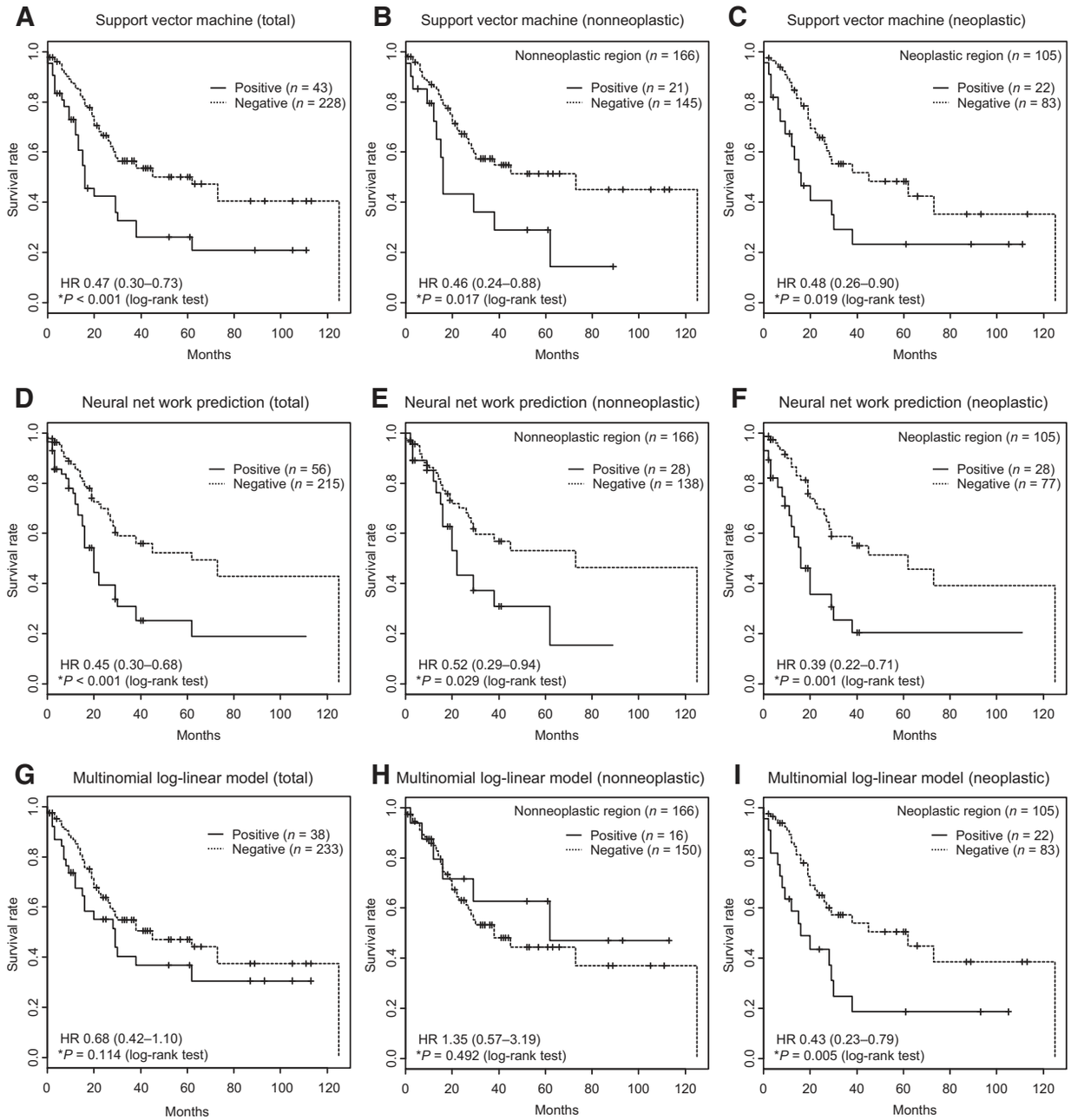

Figure 3.

Prognosis prediction by machine learning classifier in the LOOCV test. Cox proportional hazard regression analysis on a comparison between the positive and negative groups as selected by each classifier. Solid line, predicted high-risk group (positive); dashed line, other groups (negative). **A,** Classification by SVM model for all samples. **B,** Classification by SVM model in nonneoplastic tissues. **C,** Classification by SVM model in neoplastic tissues. **D,** Classification by NNET model for all samples. **E,** Classification by NNET model in nonneoplastic tissues. **F,** Classification by NNET model in neoplastic tissues. **G,** Classification by MU model for all samples. **H,** Classification by MU model in nonneoplastic tissues. **I,** Classification by MU model in neoplastic tissues.

using RT-PCR data. These mucin mRNA clustering analyses significantly separated a poor prognosis cluster. This selected cluster had higher expression levels of the three mucins than the other cluster. In our recent histologic studies, we reported that mucin gene expression, particularly MUC4, was an independent indicator of worse prognosis in PDAC (5–9). MUC2 is reported as a tumor suppressor gene, and loss of MUC2 promotes tumor progression in colon (44). However, another study showed that MUC2 expression may have a poor prognostic value for differentiated adenocarcinomas in pancreas (45). The relationship between high expression of three mucins mRNA and

Table 3. Comparison of prognosis between high-risk and other predicted by k-fold cross-validation test.

A. Support vector machine				B. Neural network				C. Multinom log-linear			
1. 3-fold CV test				1. 3-fold CV test				1. 3-fold CV test			
	P	HR	(IC_{50})		*P*	HR	(IC_{50})		*P*	HR	(IC_{50})
Total	<0.001	0.361	(0.23–0.56)	Total	<0.001	0.332	(0.22–0.50)	Total	0.002	0.500	(0.32–0.78)
Nonneoplasm	<0.001	0.344	(0.19–0.61)	Nonneoplasm	0.001	0.430	(0.25–0.73)	Nonneoplasm	0.018	0.534	(0.31–0.91)
Neoplasm	0.004	0.382	(0.19–0.75)	Neoplasm	<0.001	0.224	(0.12–0.43)	Neoplasm	0.020	0.401	(0.18–0.90)
2. 4-fold CV test				2. 4-fold CV test				2. 4-fold CV test			
	P	HR	(IC_{50})		*P*	HR	(IC_{50})		*P*	HR	(IC_{50})
Total	<0.001	0.330	(0.21–0.51)	Total	<0.001	0.332	(0.22–0.50)	Total	<0.001	0.446	(0.29–0.69)
Nonneoplasm	<0.001	0.355	(0.22–0.58)	Nonneoplasm	<0.001	0.232	(0.13–0.41)	Nonneoplasm	0.006	0.458	(0.26–0.80)
Neoplasm	0.003	0.263	(0.10–0.66)	Neoplasm	0.006	0.445	(0.25–0.80)	Neoplasm	0.017	0.426	(0.21–0.88)
3. 10-fold CV test				3. 10-fold CV test				3. 10-fold CV test			
	P	HR	(IC_{50})		*P*	HR	(IC_{50})		*P*	HR	(IC_{50})
Total	<0.001	0.329	(0.21–0.51)	Total	<0.001	0.341	(0.23–0.52)	Total	0.005	0.525	(0.33–0.83)
Nonneoplasm	0.005	0.434	(0.24–0.78)	Nonneoplasm	<0.001	0.409	(0.24–0.69)	Nonneoplasm	0.558	0.817	(0.41–1.62)
Neoplasm	<0.001	0.237	(0.12–0.46)	Neoplasm	<0.001	0.262	(0.13–0.53)	Neoplasm	<0.001	0.303	(0.16–0.58)

poor prognosis supported these recent pathologic studies. The selected cluster showed a significant difference in the nonneoplastic: neoplastic content ratio compared with the other cluster. In the neoplastic region data, the selected cluster showed a poorer prognosis than the other cluster. Interestingly, in the nonneoplastic region data, this selected cluster also showed a poorer prognosis than the other cluster. These results suggested that scientific computer methods could identify a poor prognosis using the combined data of mucin gene expression even if there was a mixture of nonneoplastic and neoplastic tissue.

A previous study revealed that an analysis of the DNA methylation status in promoters of *MUC1, MUC2*, and *MUC4* (MSE analysis of pancreatic juice samples) could differentiate between gastric-type IPMN, intestinal-type IPMN, other-type IPMN, and PDAC (33, 34). The correlation between hypomethylation of the promoter and high expression levels of mucin mRNA in pancreatic tissue was shown (28). Furthermore, we have proposed that aberrant methylation of MUC1 and MUC4 promoters are potential prognostic biomarkers for PDAC and suggested further MSE analysis of human clinical samples to determine its utility for the early diagnosis of pancreatic neoplasms and for stratifying patients with respect to modes of treatment (31). Thus, we used a methylation dataset including nonneoplastic and neoplastic pancreatic tissue. To establish whether the methylation levels of these three mucins could distinguish a poor prognosis, we performed unsupervised hierarchical clustering analysis using MSE analysis data. The clustering analysis of the three *mucin* genes' methylation data significantly separated a poor prognosis cluster. This cluster group had a higher hypomethylation level of MUC1 and MUC4 than the other clusters. Moreover, this cluster demonstrated a higher neoplastic-including ratio than the other clusters, and in neoplastic regions, this cluster showed a poorer prognosis than the other clusters. Interestingly, in the nonneoplastic region analysis, this cluster also showed a poorer prognosis than the other clusters. These results suggested that scientific computer methods could provide a model to identify a poor prognosis using the combined data of mucin gene methylation.

To evaluate whether machine learning prediction models using state-of-the-art classification algorithms such as SVM and NNET could distinguish between a poor prognosis group and others, we constructed prediction models. In LOOCV tests and k-fold cross-validation tests to evaluate prediction ability, the SVM and NNET models could significantly judge the identified high-risk group as having a poor prognosis, but the MU model could not. Multivariate and univariate analyses showed that the prediction of high-risk by SVM or NNET model was a prognostic factor significantly independent from TNM score, ASA score, preoperative chemotherapy, and comorbidities. For the neoplastic tissue analysis data, the SVM, NNET, and MU models could identify the high-risk group. Interestingly, even in the nonneoplastic tissue analysis data, the SVM and NNET model-selected high-risk group had a significantly poorer prognosis than others, similar to the neoplastic analysis. Therefore, these results suggested that the prediction models using cytological specimens and liquid biopsy samples, which are mixture of nonneoplastic and neoplastic cells, might be applicable to high-risk screening in PDAC.

When the model has high variance and low bias, such as that showing too much optimization for the training dataset, the prediction model has low prediction performance for data that has never been learned. To evaluate whether the prediction models constructed from the test dataset could detect high-risk groups in other training datasets, we split the total dataset into two groups having almost similar distribution of biological status and clinicopathologic features. The SVM and NNET classifiers could significantly distinguish the high-risk group, which has poor prognosis in the test group that has never been learned, but the MU model could not. Multivariate and univariate analyses showed that the prediction of high-risk by SVM and NNET classifiers was a prognostic factor significantly independent from TNM score, ASA score, preoperative chemotherapy, and comorbidities. These results suggested that SVM and NNET classifiers have low variance and demonstrated the high ability to distinguish a poor prognosis. Although a prospective, much larger, and multicenter randomized trial would be necessary to validate our results, it is suggested that the SVM- or NNET-based prediction models could provide a clinical risk test to predict the prognosis after surgery using *MUC1, MUC2*, and *MUC4* gene methylation analyses. Even though these SVM and NNET classifiers were a highly accurate predictor of OS, we are aware that other biomarkers may extend the precision and predictive value of the classifiers, and new markers are being identified and new techniques developed every year (46, 47). Thus, the SVM and NNET classifiers may be further improved by including additional markers.

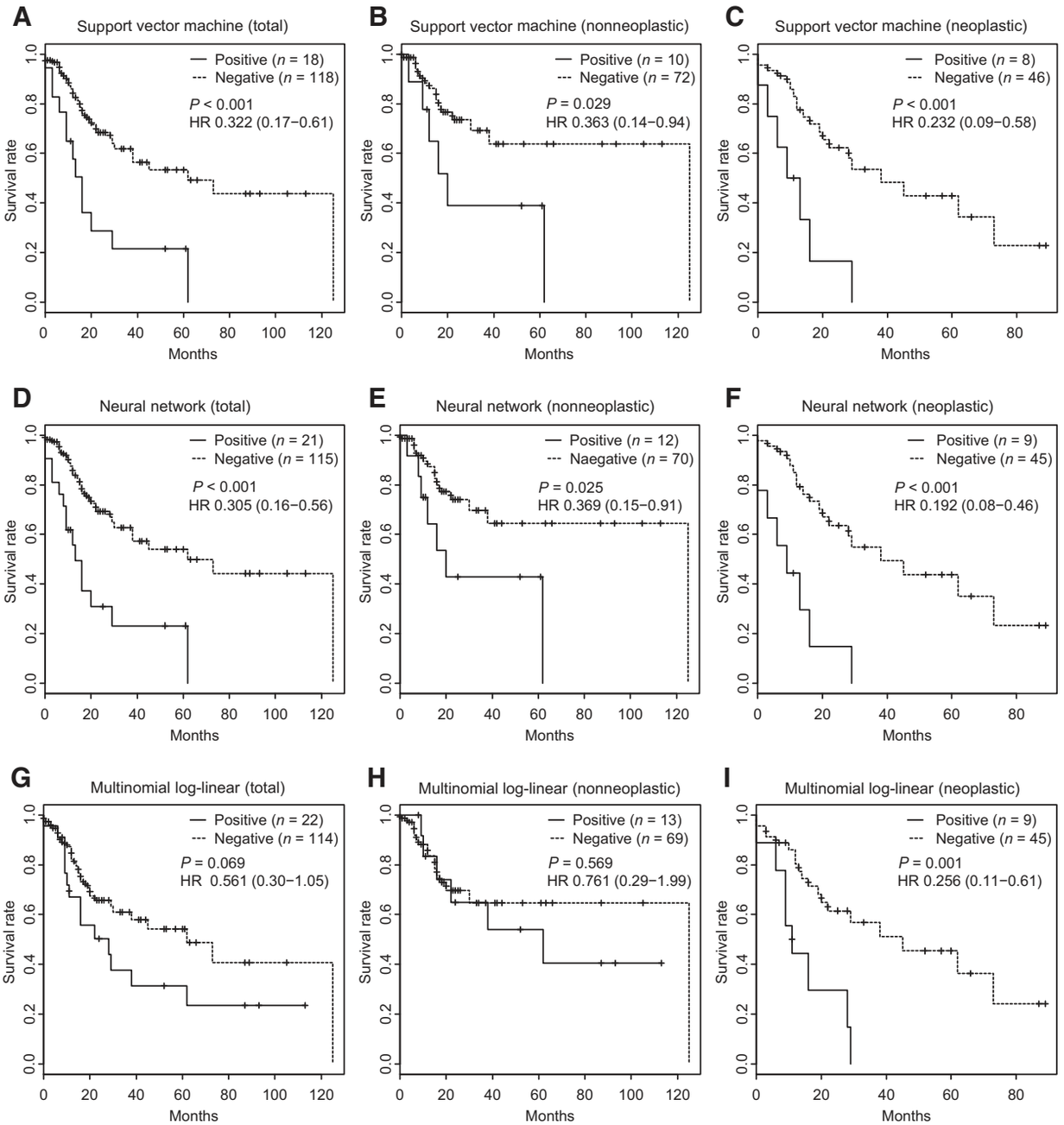

Figure 4.

Prognosis prediction by machine learning classifier in the test cohort. Cox proportional hazard regression analysis for the comparison between the positive and negative groups selected by each classifier. Solid line, predicted high-risk group (positive); dashed line, other groups (negative). **A,** Classification by SVM model for all samples. **B,** Classification by SVM model in nonneoplastic tissues. **C,** Classification by SVM model in neoplastic tissues. **D,** Classification by NNET model for all samples. **E,** Classification by NNET model in nonneoplastic tissues. **F,** Classification by NNET model in neoplastic tissues. **G,** Classification by MU model for all samples. **H,** Classification by MU model in nonneoplastic tissues. **I,** Classification by MU model in neoplastic tissues.

In summary, this study demonstrated that machine learning prediction models, based on SVM and NNET, could accurately distinguish patients with pancreatic cancer after surgery with substantially different OS. A further study is needed to expand the clinical sample spectrum, where these classifiers based on SVM or NNET might work for decision-making regarding follow-up scheduling after surgery.

Disclosure of Potential Conflicts of Interest

No potential conflicts of interest were disclosed.

Disclaimer

The funders had no role in study design, data collection and analysis, decision to publish, or preparation of the manuscript.

Authors' Contributions

Conception and design: S. Yokoyama, S. Yonezawa
Development of methodology: S. Yokoyama, S. Yonezawa
Acquisition of data (provided animals, acquired and managed patients, provided facilities, etc.): S. Yokoyama, T. Hamada, M. Higashi, K. Maemura, H. Kurahara, M. Horinouchi, T. Hiraki, M. Kornmann
Analysis and interpretation of data (e.g., statistical analysis, biostatistics, computational analysis): S. Yokoyama, T. Hamada, T. Sugimoto, S.K. Batra
Writing, review, and/or revision of the manuscript: S. Yokoyama, M. Higashi, M. Kornmann, S.K. Batra, A. Tanimoto
Administrative, technical, or material support (i.e., reporting or organizing data, constructing databases): S. Yokoyama, K. Matsuo, H. Kurahara, T. Akahane, S. Yonezawa
Study supervision: M. Higashi, S. Yonezawa, M.A. Hollingsworth, A. Tanimoto

Acknowledgments

The authors thank Orie Iwatani, Yoshie Jitoho, and Yukari Nishida for their assistance with clinical sampling and excellent technical assistance with IHC. The authors would like to thank Enago (www.enago.jp) for the English language review. This study was supported, in part, by a grant from Grants-in-Aid for Scientific Research on Scientific Research (C; 18K07019, to M. Higashi), Scientific Research (C; 18K07018, to T. Hamada), and Scientific Research (C; 18K07326, to S. Yokoyama) from the Ministry of Education, Science, Sports, Culture and Technology, Japan by the Kodama Memorial Foundation, Japan (to S. Yokoyama) and by the Pancreas Research Foundation of Japan (to S. Yokoyama).

The costs of publication of this article were defrayed in part by the payment of page charges. This article must therefore be hereby marked *advertisement* in accordance with 18 U.S.C. Section 1734 solely to indicate this fact.

Received April 14, 2019; revised August 20, 2019; accepted January 23, 2020; published first January 28, 2020.

References

1. Adamska A, Domenichini A, Falasca M. Pancreatic ductal adenocarcinoma: current and evolving therapies. Int J Mol Sci 2017;18:pii: E1338.
2. Lu D, Wang J, Shi X, Yue B, Hao J. AHNAK2 is a potential prognostic biomarker in patients with PDAC. Oncotarget 2017;8:31775–84.
3. Touchefeu Y, Le Rhun M, Coron E, Alamdari A, Heymann MF, Mosnier JF, et al. Endoscopic ultrasound-guided fine-needle aspiration for the diagnosis of solid pancreatic masses: the impact on patient-management strategy. Aliment Pharmacol Ther 2009;30:1070–7.
4. Yadav D, Lowenfels AB. The epidemiology of pancreatitis and pancreatic cancer. Gastroenterology 2013;144:1252–61.
5. Higashi M, Goto M, Saitou M, Shimizu T, Rousseau K, Batra SK, et al. Immunohistochemical study of mucin expression in periampullary adenomyoma. J Hepatobiliary Pancreat Sci 2010;17:275–83.
6. Higashi M, Yokoyama S, Yamamoto T, Goto Y, Kitazono I, Hiraki T, et al. Mucin expression in endoscopic ultrasound-guided fine-needle aspiration specimens is a useful prognostic factor in pancreatic ductal adenocarcinoma. Pancreas 2015;44:728–34.
7. Yonezawa S, Higashi M, Yamada N, Goto M. Precursor lesions of pancreatic cancer. Gut Liver 2008;2:137–54.
8. Yonezawa S, Higashi M, Yamada N, Yokoyama S, Goto M. Significance of mucin expression in pancreatobiliary neoplasms. J Hepatobiliary Pancreat Sci 2010;17:108–24.
9. Yonezawa S, Nakamura A, Horinouchi M, Sato E. The expression of several types of mucin is related to the biological behavior of pancreatic neoplasms. J Hepatobiliary Pancreat Surg 2002;9:328–41.
10. Furukawa T, Hatori T, Fujita I, Yamamoto M, Kobayashi M, Ohike N, et al. Prognostic relevance of morphological types of intraductal papillary mucinous neoplasms of the pancreas. Gut 2011;60:509–16.
11. Strobel O, Neoptolemos J, Jager D, Buchler MW. Optimizing the outcomes of pancreatic cancer surgery. Nat Rev Clin Oncol 2019;16:11–26.
12. Neoptolemos JP, Palmer DH, Ghaneh P, Psarelli EE, Valle JW, Halloran CM, et al. Comparison of adjuvant gemcitabine and capecitabine with gemcitabine monotherapy in patients with resected pancreatic cancer (ESPAC-4): a multicentre, open-label, randomised, phase 3 trial. Lancet 2017;389:1011–24.
13. Egawa S, Toma H, Ohigashi H, Okusaka T, Nakao A, Hatori T, et al. Japan pancreatic cancer registry; 30th year anniversary: japan pancreas society. Pancreas 2012;41:985–92.
14. Flejou JF. [WHO Classification of digestive tumors: the fourth edition]. Ann Pathol 2011;31:S27–31.
15. Isaji S, Kawarada Y, Uemoto S. Classification of pancreatic cancer: comparison of Japanese and UICC classifications. Pancreas 2004;28:231–4.
16. Matsuda T, Ajiki W, Marugame T, Ioka A, Tsukuma H, Sobue T, et al. Population-based survival of cancer patients diagnosed between 1993 and 1999 in Japan: a chronological and international comparative study. Jpn J Clin Oncol 2011;41:40–51.
17. Hollingsworth MA, Swanson BJ. Mucins in cancer: protection and control of the cell surface. Nat Rev Cancer 2004;4:45–60.
18. Kaur S, Kumar S, Momi N, Sasson AR, Batra SK. Mucins in pancreatic cancer and its microenvironment. Nat Rev Gastroenterol Hepatol 2013;10:607–20.
19. Kufe DW. Mucins in cancer: function, prognosis and therapy. Nat Rev Cancer 2009;9:874–85.
20. Ahmad R, Raina D, Trivedi V, Ren J, Rajabi H, Kharbanda S, et al. MUC1 oncoprotein activates the IkappaB kinase beta complex and constitutive NF-kappaB signalling. Nat Cell Biol 2007;9:1419–27.
21. Pochampalli MR, el Bejjani RM, Schroeder JA. MUC1 is a novel regulator of ErbB1 receptor trafficking. Oncogene 2007;26:1693–701.
22. Moniaux N, Andrianifahanana M, Brand RE, Batra SK. Multiple roles of mucins in pancreatic cancer, a lethal and challenging malignancy. Br J Cancer 2004;91:1633–8.
23. Mercogliano MF, De Martino M, Venturutti L, Rivas MA, Proietti CJ, Inurrigarro G, et al. TNFalpha-induced mucin 4 expression elicits trastuzumab resistance in HER2-positive breast cancer. Clin Cancer Res 2017;23:636–48.
24. Mukhopadhyay P, Lakshmanan I, Ponnusamy MP, Chakraborty S, Jain M, Pai P, et al. MUC4 overexpression augments cell migration and metastasis through EGFR family proteins in triple negative breast cancer cells. PLoS One 2013;8:e54455.
25. Tadesse S, Corner G, Dhima E, Houston M, Guha C, Augenlicht L, et al. MUC2 mucin deficiency alters inflammatory and metabolic pathways in the mouse intestinal mucosa. Oncotarget 2017;8:71456–70.
26. Yang K, Popova NV, Yang WC, Lozonschi I, Tadesse S, Kent S, et al. Interaction of Muc2 and Apc on Wnt signaling and in intestinal tumorigenesis: potential role of chronic inflammation. Cancer Res 2008;68:7313–22.
27. Yamada N, Hamada T, Goto M, Tsutsumida H, Higashi M, Nomoto M, et al. MUC2 expression is regulated by histone H3 modification and DNA methylation in pancreatic cancer. Int J Cancer 2006;119:1850–7.
28. Yamada N, Nishida Y, Tsutsumida H, Goto M, Higashi M, Nomoto M, et al. Promoter CpG methylation in cancer cells contributes to the regulation of MUC4. Br J Cancer 2009;100:344–51.
29. Yamada N, Nishida Y, Tsutsumida H, Hamada T, Goto M, Higashi M, et al. MUC1 expression is regulated by DNA methylation and histone H3 lysine 9 modification in cancer cells. Cancer Res 2008;68:2708–16.
30. Yonezawa S, Goto M, Yamada N, Higashi M, Nomoto M. Expression profiles of MUC1, MUC2, and MUC4 mucins in human neoplasms and their relationship with biological behavior. Proteomics 2008;8:3329–41.
31. Yokoyama S, Higashi M, Kitamoto S, Oeldorf M, Knippschild U, Kornmann M, et al. Aberrant methylation of MUC1 and MUC4 promoters are potential prognostic biomarkers for pancreatic ductal adenocarcinomas. Oncotarget 2016;7:42553–65.
32. Yokoyama S, Higashi M, Tsutsumida H, Wakimoto J, Hamada T, Wiest E, et al. TET1-mediated DNA hypomethylation regulates the expression of MUC4 in lung cancer. Genes Cancer 2017;8:517–27.
33. Yokoyama S, Kitamoto S, Higashi M, Goto Y, Hara T, Ikebe D, et al. Diagnosis of pancreatic neoplasms using a novel method of DNA methylation analysis of mucin expression in pancreatic juice. PLoS One 2014;9:e93760.

34. Yokoyama S, Kitamoto S, Yamada N, Houjou I, Sugai T, Nakamura S, et al. The application of methylation specific electrophoresis (MSE) to DNA methylation analysis of the 5′ CpG island of mucin in cancer cells. BMC Cancer 2012;12:67.
35. Huang S, Cai N, Pacheco PP, Narrandes S, Wang Y, Xu W. Applications of support vector machine (SVM) learning in cancer genomics. Cancer Genomics Proteomics 2018;15:41–51.
36. Ozyildirim BM, Avci M. Generalized classifier neural network. Neural Netw 2013;39:18–26.
37. Alexandros K, Alexandros S, Kurt H, Achim Z. kernlab - an S4 package for Kernel methods in R. J Stat Softw 2004;69:721–9.
38. Chen HY, Yu SL, Chen CH, Chang GC, Chen CY, Yuan A, et al. A five-gene signature and clinical outcome in non-small-cell lung cancer. N Engl J Med 2007; 356:11–20.
39. Jiang Y, Liu W, Li T, Hu Y, Chen S, Xi S, et al. Prognostic and predictive value of p21-activated kinase 6 associated support vector machine classifier in gastric cancer treated by 5-fluorouracil/oxaliplatin chemotherapy. EBioMedicine 2017; 22:78–88.
40. Wang HY, Sun BY, Zhu ZH, Chang ET, To KF, Hwang JS, et al. Eight-signature classifier for prediction of nasopharyngeal [corrected] carcinoma survival. J Clin Oncol 2011;29:4516–25.
41. Jiang Y, Xie J, Han Z, Liu W, Xi S, Huang L, et al. Immunomarker support vector machine classifier for prediction of gastric cancer survival and adjuvant chemotherapeutic benefit. Clin Cancer Res 2018;24:5574–84.
42. Ihaka R, Gentleman R. R: a language for data analysis and graphics. J Comput Graph Statist 1996;5:15.
43. Venables WN, Ripley BD. Modern applied statistics with S. New York, NY: Springer; 2012.
44. Velcich A, Yang W, Heyer J, Fragale A, Nicholas C, Viani S, et al. Colorectal cancer in mice genetically deficient in the mucin Muc2. Science 2002;295: 1726–9.
45. Takikita M, Altekruse S, Lynch CF, Goodman MT, Hernandez BY, Green M, et al. Associations between selected biomarkers and prognosis in a population-based pancreatic cancer tissue microarray. Cancer Res 2009; 69:2950–5.
46. Bernard V, Kim DU, San Lucas FA, Castillo J, Allenson K, Mulu FC, et al. Circulating nucleic acids are associated with outcomes of patients with pancreatic cancer. Gastroenterology 2019;156:108–18.
47. Krantz BA, O'Reilly EM. Biomarker-based therapy in pancreatic ductal adenocarcinoma: an emerging reality? Clin Cancer Res 2018;24:2241–50.